British Journal of Pharmacology (2001) 132, 1606–1614

www.nature.com/bjp

Functional characterization of rat submaxillary gland muscarinic receptors using microphysiometry

*,[1]Trena D. Meloy, [1]Donald V. Daniels, [1,2]Sharath S. Hegde, [1,3]Richard M. Eglen & [1]Anthony P.D.W. Ford

[1]Neurobiology Unit, Roche Bioscience, 3401 Hillview Avenue, Palo Alto, California, CA 94304, U.S.A.

1 Muscarinic cholinoceptors (MChR) in freshly dispersed rat salivary gland (RSG) cells were characterized using microphysiometry to measure changes in acidification rates. Several non-selective and selective muscarinic antagonists were used to elucidate the nature of the subtypes mediating the response to carbachol.

2 The effects of carbachol ($pEC_{50} = 5.74 \pm 0.02$ s.e.mean; $n = 53$) were highly reproducible and most antagonists acted in a surmountable, reversible fashion. The following antagonist rank order, with apparent affinity constants in parentheses, was noted: 4-DAMP (8.9) = atropine (8.9) > tolterodine (8.5) > oxybutynin (7.9) > S-secoverine (7.2) > pirenzepine (6.9) > himbacine (6.8) > AQ-RA 741 (6.6) > methoctramine (5.9).

3 These studies validate the use of primary isolated RSG cells in microphysiometry for pharmacological analysis. These data are consistent with, and extend, previous studies using alternative functional methods, which reported a lack of differential receptor pharmacology between bladder and salivary gland tissue.

4 The antagonist affinity profile significantly correlated with the profile at human recombinant muscarinic M_3 and M_5 receptors. Given a lack of antagonists that discriminate between M_3 and M_5, definitive conclusion of which subtype(s) is present within RSG cells cannot be determined.
British Journal of Pharmacology (2001) **132,** 1606–1614

Keywords: Muscarinic receptors; microphysiometry; rat submaxillary gland; muscarinic antagonists

Abbreviations: AQ-RA 741, 11-[[4-[4-(diethylamino)butyl]-1-piperidinyl]acetyl]-5,11-dihydro-6H-pyrido(2,3-b)(1,4)-benzodiazepine-6-one; CHO K1, Chinese hamster ovary cells; 4-DAMP, 4-diphenylacetoxy-N-methylpiperidine; MChR, muscarinic cholinoceptor; RSG, rat submaxillary gland; *p*-F-HHSiD, para-fluoro-hexahydro-sila-difenidol; SSQ, sum of squares of differences ($\sum (x-y)^2$)

Introduction

Muscarinic cholinoceptor (MChR) antagonists have therapeutic utility in overactive bladder. However, several side effects associated with these therapies, including dry mouth and blurred vision, limit their applicability (Owens & Karram, 1998; Yarker *et al*., 1995; Norton *et al*., 1994). Consequently, the identification of novel compounds that are selective for MChR subtype(s) in urinary bladder over those mediating salivation may provide a significant advance over current therapies.

There are five recognized muscarinic receptor subtypes (M_1 to M_5), each possessing different distributions and functions (Caulfield, 1993). M_1, M_3, and M_5 receptors positively couple to phospholipase C, while muscarinic M_2 and M_4 receptors negatively couple to adenylyl cyclase. Although physiological functions have been proposed for M_1 to M_4, they are ill defined for the M_5 subtype (Eglen & Nahorski, 2000). Of the five muscarinic receptors, M_2 and M_3 are highly abundant in smooth muscle tissue (Eglen *et al*., 1997). Previous pharmacological studies, functional and binding, in salivary gland suggested only a role for muscarinic M_3 receptors in the regulation of salivation (Dai *et al*., 1991; Laniyonu *et al*., 1990; Moriya *et al*., 1999).

Rat submaxillary gland has frequently been studied for pharmacological characterization of the MChRs involved in secretion by examining the following assays: ^{86}rubidium efflux (Bovell *et al*., 1989), calcium mobilization (Hurley & Brinck, 1992; Valdez & Turner, 1991), inositol phosphates accumulation (Laniyonu *et al*., 1990; Abdallah *et al*., 1992), and inhibition of adenylyl cyclase activity (Dai *et al*., 1991; Laniyonu *et al*., 1990; Abdallah *et al*., 1992). While these approaches offer some insight into cellular function in rat submaxillary gland, they generally lack a robust method to determine antagonist affinity and thus characterize the muscarinic subtype. An alternative approach is to employ a functional response in intact cells by using microphysiometry. In the current studies, the Cytosensor® microphysiometer (Molecular Devices Corp.) was utilized to operationally characterize the MChR subtype(s) responsible for the changes in the total metabolic activity, *in vitro*, of freshly dispersed submaxillary gland cells from the rat.

Preliminary reports of these findings have been presented to Experimental Biology 98 (Meloy *et al*., 1998).

*Author for correspondence at: Roche Bioscience, R2-101, 3401 Hillview Avenue, Palo Alto, CA 94304, U.S.A.
E-mail: trena.meloy@roche.com
Current addresses: [2]Advanced Medicine, Inc., 901 Gateway Blvd, South San Francisco, CA 94080, U.S.A.; [3]DiscoveRx, 42501 Albrae St., Suite 100, Fremont, CA 94538, U.S.A.

Methods

Microphysiometer running medium

Modified RPMI 1640 medium lacking sodium bicarbonate (Molecular Devices Corp., Sunnyvale, CA, U.S.A.) was used in these studies. Supplied powder was dissolved in Nanopure water and titrated up to pH 7.40 with 0.1 M and 1 M NaOH. The medium was sterile-filtered using Nalgene tissue culture units (1 L, 0.2 μM; Nalge Nunc International, Rochester, NY, U.S.A.).

Cell preparation and microphysiometry procedure

Male Sprague-Dawley rats (250–600 g) from Charles River Laboratories (Wilmington, MA, U.S.A.) were asphyxiated with CO_2 and decapitated. Submaxillary (submandibular) glandular tissue was dissected and placed on a McIlwain Tissue Chopper set at 350 μm, turned 90°, chopped, turned 90°, and chopped for a third time. Two glands per experiment were digested with 1 mg ml^{-1} collagenase (Sigma Chemical Co., St. Louis, MO, U.S.A.) in 50 ml Ham's F-12 medium (GibcoBRL, Gaithersburg, MD, U.S.A.) at 37°C for 1 h with frequent shaking. The cells were filtered through a Cellector tissue sieve (40 mesh screen), washed twice with F-12 medium, centrifuged at 1200 r.p.m. between washes, and resuspended in 20 ml F-12 medium. The cells were then counted using a hemacytometer. Approximately 2×10^6 cells were centrifuged and resuspended in 100 μl low-buffered RPMI (running medium), pH 7.4 plus 50 μl of melted agarose cell entrapment medium (Molecular Devices Corp., Sunnyvale, CA, U.S.A.). A 7 μl aliquot of the cell/agarose suspension was dotted onto the centre of a capsule cup (pre-chilled at 4°C for >15 min) in a transwell capsule plate (3 μm pore size; Corning Costar Corp., Cambridge, MA, U.S.A.) and allowed to air dry 10 min before addition of the spacer and RPMI buffer. For treatment with test compounds in the microphysiometer, a transwell spacer and insert (Molecular Devices Corp., Sunnyvale, CA, U.S.A.) were added to each transwell capsule, and the capsules placed in sensor chambers (one capsule per chamber). Eight sensor chambers were used per experiment. The sensor chambers were loaded onto the microphysiometer and running medium was pumped through the transwell capsules at a rate of 100 μl min^{-1} (microphysiometer setting = 50%) with a peristaltic pump. Test compound pump cycle, exposure times, recovery intervals, and acceptable baseline pH accumulation rates were empirically determined for the rat submaxillary gland cells. Total pump cycle time was 2 min, which included 53 s pump-off period, during which the acidification rate was measured for 45 s (i.e. the Get Rate). RSG cells were exposed to carbachol for 65 s beginning 55 s after pump-on began (12 s before pump-off began), and then allowed to recover during a 28 min 55 s wash interval before the next exposure to compound. RSG cells were first allowed to equilibrate with running medium on the microphysiometer for approximately 2 h, then with antagonist or running medium for an additional 17 min before exposure to carbachol.

Experimental protocol and measurement of cellular responses

Cell chambers were exposed to increasing concentrations of agonist in the presence or absence of antagonist at a fixed concentration. Agonist additions to the cells were made with valve switches during perfusion. The maximum metabolic acidification rate at each concentration was recorded and expressed as per cent change over the basal acidification rate. All measurements were made using Cytosoft (Molecular Devices Corp., Sunnyvale, CA, U.S.A.) software provided with the Cytosensor® microphysiometer (McConnell *et al*., 1992). Briefly, a silicon chip, located at the bottom of the sensor chamber, functioned as an extremely sensitive detector of hydrogen ions. A light emitting diode (LED) positioned below the sensor chamber allowed pH readings in the centre of the cell capsule to be made continuously throughout the pump cycle (see above), and pH readings recorded and displayed on the computer as 'Raw Data' in millivolt (mV) units. The data collected when the pumps were off were fitted to a straight line and the slope of the line was plotted as the acidification rate ('Rate Data' in μV s^{-1} units). All data were recorded throughout the experiment using the Cytosoft software package. After data collection, selected segments of the acidification rates were normalized using Cytosoft.

Changes in cellular metabolic activity in response to muscarinic agonist (carbachol), in the presence or absence of antagonist, were expressed as Acidification Response (% above basal). Normalized Rate Data were exported to a spreadsheet program (Microsoft Excel) and analysed using the following equation: Acidification Response [% above basal] = $(CP_{rate} - Baseline_{rate}) \times (Baseline_{rate} \times 100)^{-1}$. CP_{rate} indicates the normalized peak metabolic Rate Data point after exposure to test compound (Chosen Point) and $Baseline_{rate}$ indicates the normalized average of the three Rate Data points immediately preceding exposure to test compound.

Data analysis

Rate Data were analysed to construct concentration-effect (E [A]$^{-1}$) curves by iterative curve fitting to a four-parameter logistic equation to determine minimum, maximum, pEC_{50} and Hill slope (n_H) values. Kaleidagraph software was used to fit data to the general logistic function: $E = basal + [E_m \times A^{nH}] \times [(A^{nH} + [A]_{50}{}^{nH})]^{-1}$ for agonist stimulation curves. Schild plots were constructed to study the nature of antagonism over a wide range of concentrations. pA_2 values were estimated from x-intercept, and pK_B values, where appropriate, were estimated by constraining regression line slope to one (assuming Schild slope was not significantly different from one; Jenkinson *et al*., 1995).

The correlation coefficient, r value (ranging from −1 to 1), reflects the degree of linear relationship between two variables. The larger the absolute r value, the stronger the linear association between the two variables. $\sum (x-y)^2$ is the sum of squares of differences in affinity estimates for each plot, and describes, in relative terms, to what degree two data sets differ.

Statistical analysis

Data are expressed as mean and standard error of the mean (s.e.mean) for each compound tested (3–6 independent experiments; 5–16 replicates).

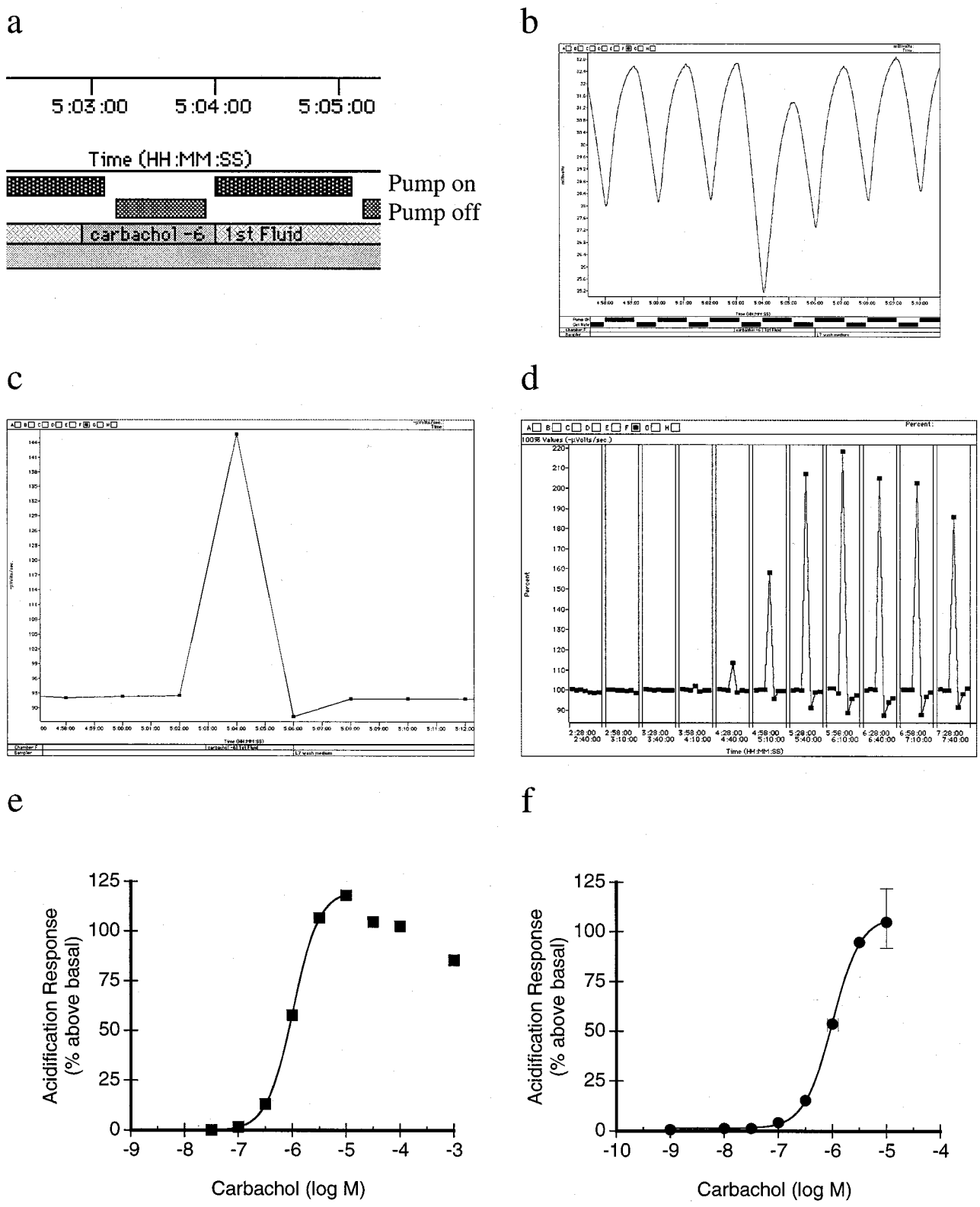

Figure 1 Representative experiment performed using carbachol-stimulated rat submaxillary gland (RSG) cells in microphysiometer. Sample of pump cycle (a), raw data (b), rate data (c), normalized segments (d), and resulting curve (e) generated from a single sensor chamber exposed to increasing concentrations of carbachol (10^{-9} to 10^{-5} M). (f) Mean of seven individual carbachol curves from a single experiment ($pEC_{50} = 5.99 \pm 0.10$ (s.d.), max $= 107 \pm 15\%$ (s.d.)).

Compounds used

Carbachol, atropine and oxybutynin were purchased from Sigma Chemical Co. (St. Louis, MO, U.S.A.). 4-DAMP (4-diphenylacetoxy-N-methylpiperidine), methoctramine, pirenzepine and *p*-F-HHSiD (para-fluoro-hexahydro-sila-difenidol) were purchased from RBI (Natick, MA, U.S.A.). Himbacine was kindly provided by Professor W.C. Taylor (University of Sydney, New South Wales, Australia). AQ-RA 741 (structure) was a gift from Boehringer Ingelheim Pharmaceuticals Inc., U.S.A.. Darifenacin and zamifenacin were provided by Pfizer Central Research (Kent, U.K.). Remaining compounds were synthesized in the Medicinal Chemistry Group, Neurobiology Unit, Roche Bioscience (Palo Alto, CA, U.S.A.). All stock solutions of compounds were dissolved in running medium, with the exceptions of darifenacin and zamifenacin, which were dissolved in DMSO (100% in 10^{-2} M stock solution). All serial dilutions were performed using running medium.

Results

Measurement of responses

Muscarinic receptor activation in response to carbachol was assessed as changes in the acidification rate during the pump-off period of the experiment. Figure 1a–e illustrates the progression from Raw Data to Rate Data obtained in a single channel. Exposure of the cells to agonist occurred 12 s before the peristaltic pump was turned off during a single pump cycle (Figure 1a). Data were gathered during the pump-off period, when the metabolic activity of the cells acidified the extracellular medium. The drop in pH was measured as a decrease in μV over time, where 1 μV s^{-1} was approximately 0.001 pH min^{-1} (Figure 1b) (McConnell *et al*., 1992). The data gathered during the pump-off period were fitted to a straight line using a least-squares method, with the resulting slope of the line reported as the acidification rate (Figure 1c). Acidification rate data for exposure to carbachol were normalized to baseline rate data (Figure 1d) at the conclusion of the experiment, and subsequently exported to a graphing program to generate concentration-effect (E $[A]^{-1}$) curves (Figure 1e).

Figure 1f shows the mean E $[A]^{-1}$ curve generated with data from seven separate sensor chambers in one experiment. Carbachol produced concentration-dependent changes in cellular acidification with a potency (pEC_{50}) of 5.99 ± 0.03 and a maximum of $107 \pm 5\%$.

Measurement of apparent antagonist affinities

Carbachol concentration-effect curves were constructed in the presence of increasing concentrations of muscarinic antagonists. In this manner, rightward, concentration-dependent shifts of the curves allowed for the determination of pA_2 and pK_B values (Table 1).

Figure 2 contains representative antagonist curve shifts using himbacine (0.3–5 μM). In the presence of antagonist, there was no reduction in basal rate seen during the antagonist equilibration phase, suggesting a lack of inverse agonism or the presence of endogenous agonist in these preparations. The presence of antagonist resulted, in most cases, in the rightward, parallel shift of the concentration-effect curves. Deviations from this occurred with darifenacin, *p*-F-HHSiD, and zamifenacin.

Figure 3 contains Schild plot analysis for the 12 antagonists tested (4-DAMP, AQ-RA 741, atropine, darifenacin, himbacine, methoctramine, oxybutynin, *p*-F-HHSiD, pirenzepine, S-secoverine, tolterodine, and zamifenacin; $n = 5-16$). pK_B determinations were made for the nine compounds in which the Schild slopes did not differ significantly from one (4-DAMP, AQ-RA 741, atropine, himbacine, methoctramine, oxybutynin, pirenzepine, S-secoverine, and tolterodine). However, for darifenacin, *p*-F-HHSiD, and zamifenacin, the slopes were 0.47 ± 0.21, 1.19 ± 0.04 and 1.40 ± 0.13, respectively, and pK_B values could not be calculated. In addition, there was significant suppression of the curve maxima in the presence of darifenacin, precluding rigorous Schild analysis. Table 1 contains the pK_B, pA_2, Schild slope and r values, where appropriate.

Table 1 Antagonist affinity estimates (pK_B, pA_2) for muscarinic antagonists in rat submaxillary gland using microphysiometry

Compound	pK_B mean ± s.e.mean	pA_2	Schild slope (95% CI)†	r value
4-DAMP	8.88 ± 0.05	8.93	0.95 (0.74, 1.16)	0.97
AQ-RA 741	6.63 ± 0.02	6.65	0.98 (0.87, 1.08)	0.99
Atropine	8.85 ± 0.04	8.73	1.07 (0.95, 1.20)	0.99
Himbacine	6.82 ± 0.04	6.98	0.84 (0.59, 1.10)	0.96
Methoctramine	5.90 ± 0.09	5.73	1.26 (0.53, 1.99)	0.95
Oxybutynin	7.94 ± 0.06	7.78	1.14 (0.94, 1.35)	0.98
Pirenzepine	6.85 ± 0.04	6.96	0.86 (0.66, 1.05)	0.96
S-secoverine	7.18 ± 0.03	7.15	1.05 (0.96, 1.14)	0.99
Tolterodine	8.51 ± 0.04	8.45	1.06 (0.86, 1.27)	0.99
Darifenacin	n.d.	10.74	0.47 (0.02, 0.96)*	0.62
p-F-HHSiD	n.d.	7.14	1.19 (1.09, 1.30)*	1.00
Zamifenacin	n.d.	7.68	1.40 (1.09, 1.71)*	0.97

pK_B is mean of individual determinations ($n = 5-16$). n.d. = pK_B affinity estimates were not determined for this compound as the Schild slope was significantly different from one* ($P < 0.05$). †95% confidence interval for the slope (low, high).

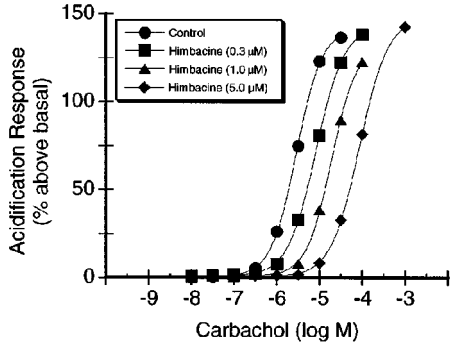

Figure 2 Acidification response in freshly dispersed RSG cells to carbachol in the absence and presence of himbacine. Data shown are from a single representative experiment performed with single point determinations. Each curve represents a concentration-effect curve generated from a single sensor chamber (one individual determination). Individual determinations ($n = 5-16$) were repeated in at least three independent experiments.

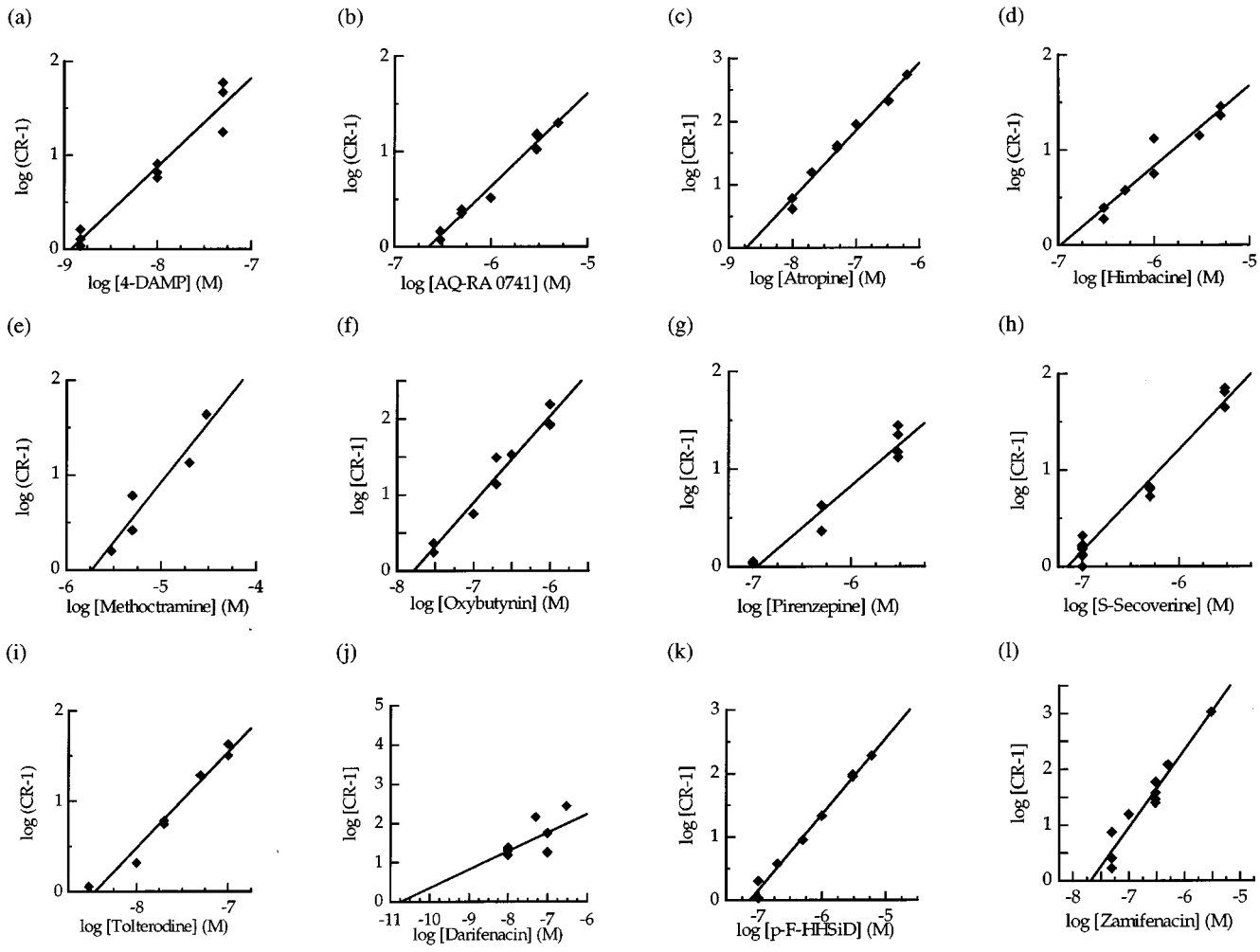

Figure 3 Schild analysis for (a) 4-DAMP, (b) AQ-RA 741, (c) atropine, (d) himbacine, (e) methoctramine, (f) oxybutynin, (g) pirenzepine, (h) S-secoverine, (i) tolterodine, (j) darifenacin, (k) *p*-F-HHSiD, and (l) zamifenacin. Data shown are single point determinations from individual curve shifts (single chamber, $n=5-16$). The data shown on the Schild plot were fit to a straight line using a least-squares method (linear regression). The average of the individual determinations ± s.e.mean are reported in Table 1.

Correlation plots (Figure 4) were constructed using affinity estimates from Table 2 to demonstrate the relationship between binding affinity estimates (pK_i) generated at human recombinant muscarinic receptors (M_1 to M_5) expressed in CHO K1 cells, and functional affinity estimates (pK_B) generated in the present study. Each plot contains the line of identity ($y=x$) indicated by the solid line and the SSQ value. A correlation between affinity estimates for muscarinic receptor(s) present in RSG and cloned M_1, M_3 and M_5 receptors was shown in these plots.

Discussion

Muscarinic receptor antagonists effectively control symptoms of overactive bladder, but their side effects, particularly dry mouth, lead to increased fluid intake and subsequent exacerbation of bladder overactivity. Elucidation of potential differences between MChR subtypes in bladder and salivary gland may enable the discovery of novel, selective therapies with reduced side effects. Although several methods have been applied in the search for such tissue differences, none have yielded conclusive results. In the present study, we have developed an *in vitro* assay using the Cytosensor® microphysiometer to characterize the MChR(s) in freshly dispersed rat submaxillary (submandibular) gland (RSG) cells.

Utility of microphysiometry in muscarinic RSG receptor characterization

Microphysiometry is an attractive alternative to previous methods, and we report here the first use of this technique in receptor characterization of freshly dispersed RSG cells. While the quantitative characterization of muscarinic subtypes *in vitro* using bladder smooth muscle is feasible, such analysis of salivary gland function has proven more challenging. In these studies, we show that microphysiometry provides a quantitative profile of cellular response to MChR antagonists and, with few exceptions, is robust and practical. Most studies of MChR characterization of salivary gland have involved measurements of such endpoints as ^{86}Rb efflux, calcium influx, inositol phosphates accumulation, and inhibition of adenylyl cyclase activity upon exposure of the

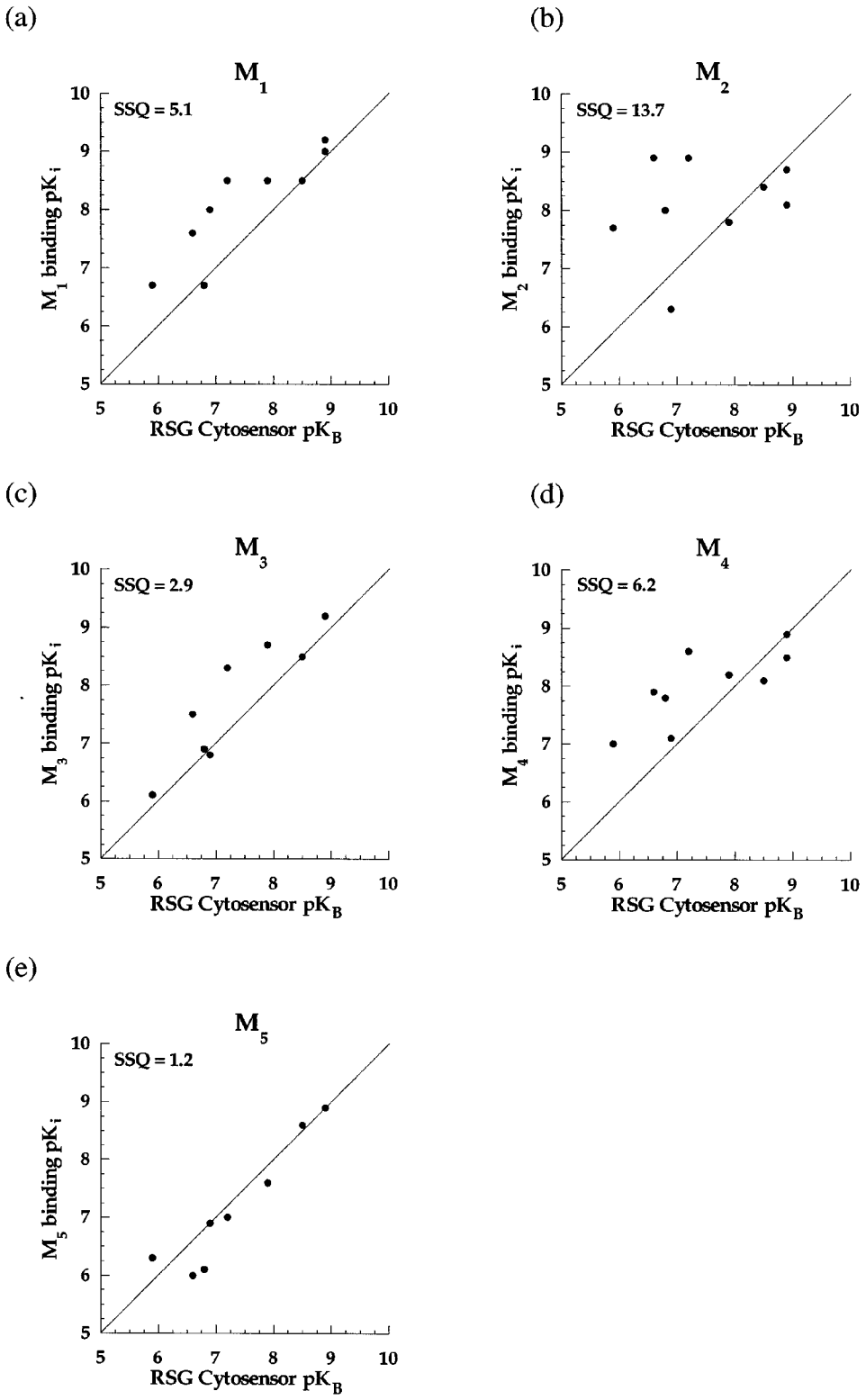

Figure 4 Correlation plots showing relationship of binding affinity data (pK_i) generated at human recombinant muscarinic (a) M_1, (b) M_2, (c) M_3, (d) M_4 and (e) M_5 expressed in CHO K1 cells with functional affinity estimates (pK_B) generated in the RSG. In each plot, a solid line indicates the line of identity ($y=x$). SSQ = sum of squares of differences between affinity estimates ($\sum(x-y)^2$).

cells to known MChR antagonists. None of these methods are either sufficiently robust or relevant to offer unambiguous pharmacological characterization that is reflective of total metabolic activity of the target cells. For example, ^{86}Rb efflux and calcium influx determinations measure a downstream effect of a compound on target cells, which has been proposed to reflect saliva secretion. However, ^{86}Rb efflux suffers from poor data fidelity due to a small signal to noise

Table 2 Antagonist affinity estimates (pK_B) derived from microphysiometry studies in RSG compared with radioligand binding data (pK_i) at cloned human muscarinic M_1–M_5 receptors

Compound	*RSG* pK_B	M_1 pK_i	M_2 pK_i	M_3 pK_i	M_4 pK_i	M_5 pK_i
4-DAMP‡	8.9	9.2	8.1	9.2	8.5	8.9
AQ-RA 741†	6.6	7.6	8.9	7.5	7.9	6.0
Atropine‡	8.9	9.0	8.7	9.2	8.9	8.9
Himbacine**	6.8	6.7	8.0	6.9	7.8	6.1
Methoctramine**	5.9	6.7	7.7	6.1	7.0	6.3
Oxybutynin‡	7.9	8.5	7.8	8.7	8.2	7.6
Pirenzepine**	6.9	8.0	6.3	6.8	7.1	6.9
S-Secoverine†	7.2	8.5	8.9	8.3	8.6	7.0
Tolterodine*	8.5	8.5	8.4	8.5	8.1	8.6
Sum of squares (vs RSG)		5.1	13.7	2.9	6.2	1.2

pK_B is mean of individual determinations ($n = 5–16$). Binding estimates are from *Eglen *et al*., 1997, **Loury *et al*., 1999 and †Choppin *et al*., 1999. ‡Unpublished data provided by D.N. Loury and D.W. Bonhaus (Roche Bioscience, Palo Alto, U.S.A.).

ratio, and thus it is difficult to quantitatively differentiate antagonist affinities (Bovell *et al*., 1989). Calcium influx-based approaches measure the endpoint of only one metabolic event in response to an effector, rather than measuring a global metabolic response. Inositol phosphates accumulation and inhibition of adenylyl cyclase activity are assays that only measure a single second-messenger, thus they represent biased functional response signals that are receptor-specific.

All techniques relying on functional analogy have drawbacks, and microphysiometry is no exception. Some difficulties relate to the physiochemical properties of the antagonist as well as its known pharmacological properties. We found that compounds such as darifenacin, *p*-F-HHSiD, and zamifenacin had Schild slopes significantly different from one. This finding could be due to compound accumulation within the chamber, to compound sticking to the peristaltic tubing, or to pseudo-irreversible antagonism. With darifenacin, we found a decreased E_{max} in agonist curves with increasing concentration of this compound. Further studies with multiple exposures to agonist after a single exposure to darifenacin (data not shown) revealed that the drug washed out of the system very slowly, displaying typical pseudo-irreversible antagonism. Thus, for these compounds, pK_B values could not be estimated and their utility in our screen was limited.

Our studies with microphysiometry also identified some technical limitations of this method that were not universal and affected a minority of responses. For example, we were not able to add agonist too close to the scheduled pump-off time because peristaltic pump speeds varied slightly among chambers. However, in studies where a resolution time of greater than 5 s can be tolerated, this effect becomes less significant. Some drawbacks could also be attributed to the software used in our analyses. For example, the optimization software used (Cytosoft) did not enable extraction of all experimental data for the entire duration of the experiment. In addition, the software did not allow us to select the greatest change in acidification during the Get Rate (i.e. greatest slope), reporting only the value of the slope for the entire Get Rate period.

Another area of note was the rate of data capture that the microphysiometer used, which could limit the quantity of usable data. For example, when carbachol (a rapidly acting agonist) was used at the higher concentrations (Figure 1e), there was a characteristic fall-off in response because the equipment was not able to capture data quickly enough. Since the response recorded for these higher concentrations was not an accurate reflection of the true response to the agonist, these data points were omitted from further analysis. Although we describe this observation with RSG cells, this type of response has been reported by others to occur with other targets, including MChRs transfected into CHO K1 cells (Baxter *et al*., 1994). Thus, we were compelled to select a sub-maximal stimulus level to collect linear data. This decision represents a need for compromise in data acquisition through microphysiometry, because with some agonists the Get Rate may be found to begin too soon at low concentrations of agonist and too late at high concentrations due to physical limitations in delivering compound to the chamber. Despite these noted limitations, we found microphysiometry to be a worthwhile and advantageous method in studies of this type.

Assessment of the muscarinic receptors in RSG

Concentration-effect curves to carbachol established in the absence and presence of muscarinic antagonists, resulted in monophasic, parallel, surmountable shifts (except darifenacin, *p*-F-HHSiD, and zamifenacin) consistent with competitive antagonism at a single site. Additionally, regression analysis revealed linear Schild slopes providing no evidence for involvement of more than one receptor subtype. Currently, there are few muscarinic antagonists that are clearly selective for one subtype over the remaining four. Therefore, it is critical to use several selective compounds to determine the subtype(s) present within a tissue. Previous studies in salivary gland tissue have typically used less than five different antagonists to characterize the functional MChR(s) present within the tissue.

In this study, we attempted to distinguish the functional MChR subtype(s) present in RSG cells. The sums of squares (SSQ) of the differences between RSG microphysiometer pK_B and binding pK_i affinity estimates were generated as a mathematical representation of the similarity (or difference) between the two affinity values. The smaller the SSQ value, the smaller the difference between RSG microphysiometer pK_B and binding pK_i data. As shown in the correlation plots, the data in the present study demonstrate the close resemblance that M_1, M_3 and M_5 binding affinity values have to pK_B values obtained for RSG microphysiometry data (Figure 4). However, since key muscarinic antagonists selective for M_1 (methoctramine $pK_i = 6.7$; pirenzepine $pK_i = 8.0$) displayed poor affinity in RSG cells (methoctramine $pK_B = 5.9$, pirenzepine $pK_B = 6.9$), the data suggest the function of either muscarinic M_3 or M_5 receptor.

Schild slopes equivalent to one (for most compounds) and the lack of any inflection point in Schild analysis suggest the presence of only one functional receptor subtype rather than a combination of subtypes. Given the current lack of pharmacological tools able to discriminate further between M_3 and M_5 receptor subtypes, it is not definitively clear which subtype functions predominantly within the rat

salivary gland. Our results echoed previously reported literature values, which reported a lack of differential receptor subtype(s) between bladder (Hegde *et al*., 1997; Longhurst *et al*., 1995) and salivary gland tissue (Dai *et al*., 1991; Laniyonu *et al*., 1990; Moriya *et al*., 1999) as determined in functional and binding studies.

In the present study the affinity constants for the compounds studies were representative of both subtypes. This may suggest either that the nature of the receptor, and thus its pharmacology, was affected during tissue preparation or that both subtypes were detected by the microphysiometry technique. Numerous lines of data (see Caulfield, 1993, for review) indicate that M_3 receptors are expressed in rat salivary gland. In addition, data from knockout mice for the M_3 receptor (Matsui *et al*., 2000) show impaired salivary secretion upon stimulation with pilocarpine. Interesting, also, are preliminary data from Yeomans *et al*. (1999) indicating that mice with a null mutation in the M_5 gene have a reduction in pilocarpine-stimulated salivation. This may suggest a functional role of the M_5 subtype in murine tissue and supports radioligand binding data in rat tissue (Flynn *et al*., 1997) also demonstrating expression of the subtype.

The pharmacological differentiation between the MChR playing the predominant physiological role in bladder and salivary function remains a challenge and a prerequisite to the discovery of therapies that offer symptomatic control for bladder overactivity with fewer side effects. The current studies indicate that most likely one subtype functions within rat submaxillary gland, and correlation data suggest the MChR subtype is pharmacologically consistent with either M_3 or M_5. Because known muscarinic antagonists have affinity values that differ little between M_3 and M_5 (Buckley *et al*., 1989; Dörje *et al*., 1991; Jones *et al*., 1991; Watson *et al*., 1999; Eglen & Nahorski, 2000), new compounds that demonstrate improved selectivity for MChR subtypes may prove to be better tools for discrimination and may be optimal candidates for novel therapeutics.

The authors would like to thank Dr Nikki Watson for her valuable comments and discussions, Dana Loury and Dr Doug Bonhaus for binding data from cloned human muscarinic receptors, and Dr Ondine Callan for statistical analysis.

References

ABDALLAH, E.A., JETT, D.A., ELDEFRAWI, M.E. & ELDEFRAWI, A.T. (1992). Differential effects of paraoxon on the M_3 muscarinic receptor and its effector system in rat submaxillary gland cells. *J. Biochem. Toxicol.,* **7,** 125–132.

BAXTER, G.T., YOUNG, M.L., MILLER, D.L. & OWICKI, J.C. (1994). Using microphysiometry to study the pharmacology of exogenously expressed M_1 and M_3 muscarinic receptors. *Life Sci.,* **55,** 573–583.

BOVELL, D.L., ELDER, H.Y., PEDIANI, J.D. & WILSON, S.M. (1989). Potassium ($^{86}Rb^+$) efflux from the rat submandibular gland under sodium-free conditions in vitro. *J. Physiol.,* **416,** 503–515.

BUCKLEY, N.J., BONNER, T.I., BUCKLEY, C.M. & BRANN, M.R. (1989). Antagonist binding properties of five cloned muscarinic receptors expressed in CHO-K1 cells. *Mol. Pharmacol.,* **35,** 469–476.

CAULFIELD, M.P. (1993). Muscarinic receptors – characterization, coupling and function. *Pharmacol. Therapeut.,* **58,** 319–379.

CHOPPIN, A., LOURY, D.N., WATSON, N., HEGDE, S.S. & EGLEN, R.M. (1999). S-Secoverine: a defining ligand in muscarinic M_5 receptor characterization. *Br. J. Pharmacol.,* **128,** 33P.

DAI, Y.S., AMBUDKAR, I.S., HORN, V.J., YEH, C.K., KOUSVELARI, E.E., WALL, S.J., LI, M., YASUDA, R.P., WOLFE, B.B. & BAUM, B.J. (1991). Evidence that M_3 muscarinic receptors in rat parotid gland couple to two second messenger systems. *Am. J. Physiol.,* **261,** C1063–C1073.

DÖRJE, F., WESS, J., LAMBRECHT, G., TACKE, R., MUTSCHLER, E. & BRANN, M.R. (1991). Antagonist binding profiles of five cloned human muscarinic receptor subtypes. *J. Pharmacol. Exp. Ther.,* **256,** 727–733.

EGLEN, R.M., BONHAUS, D.W., CALIXTO, J.J., CHOPPIN, A., LEUNG, E., LOEB, M., LOURY, D., MOY, T., WILDA, M. & HEGDE, S.S. (1997). Characterization of the interaction of tolterodine at muscarinic receptor subtypes in vitro and in vivo. *Br. J. Pharmacol.,* **120,** 63P.

EGLEN, R.M. & NAHORSKI, S.R. (2000). The muscarinic M_5 receptor: a silent or emerging subtype? *Br. J. Pharmacol.,* **130,** 13–21.

FLYNN, D.D., REEVER, C.M. & FERRARI-DILEO, G. (1997). Pharmacological strategies to selectively label and localize muscarinic receptor subtypes. *Drug Devel. Res.,* **40,** 104–116.

HEGDE, S.S., CHOPPIN, A., BONHAUS, D., BRIAUD, S., LOEB, M., MOY, T.M., LOURY, D. & EGLEN, R.M. (1997). Functional role of M_2 and M_3 muscarinic receptors in the urinary bladder of rats *in vitro* and *in vivo*. *Br. J. Pharmacol.,* **120,** 1409–1418.

HURLEY, T.W. & BRINCK, R.W. (1992). Differential regulation of agonist-stimulated Ca^{2+} influx in acini of rat pancreas and submandibular gland. *Arch. Oral Biol.,* **37,** 763–769.

JENKINSON, D.H., BARNARD, E.A., HOYER, D., HUMPHREY, P.P., LEFF, P. & SHANKLEY, N.P. (1995). International Union of Pharmacology Committee on Receptor Nomenclature and Drug Classification. IX. Recommendations on terms and symbols in quantitative pharmacology. *Pharmacol. Rev.,* **47,** 255–266.

JONES, S.V.P., HEILMAN, C.J. & BRANN, M.R. (1991). Functional responses of cloned muscarinic receptors expressed in CHO-K1 cells. *Mol. Pharmacol.,* **40,** 242–247.

LANIYONU, A., SLIWINSKI-LIS, E. & FLEMING, N. (1990). Muscarinic M_3 receptors are coupled to two signal transduction pathways in rat submandibular cells. *Eur. J. Pharmacol.,* **188,** 171–174.

LONGHURST, P.A., LEGGETT, R.E. & BRISCOE, J.A.K. (1995). Characterization of the functional muscarinic receptors in the rat urinary bladder. *Br. J. Pharmacol.,* **116,** 2279–2285.

LOURY, D.N., HEGDE, S.S., BONHAUS, D.W. & EGLEN, R.M. (1999). Ionic strength of assay buffers influences antagonist binding affinity estimates at muscarinic M_1-M_5 cholinoceptors. *Life Sci.,* **64,** 557.

MATSUI, M., MOTOMURA, D., KARASAWA, H., FUJIKAWA, T., JIANG, J., KOMIYA, Y., TAKAHASHI, S. & TAKETO, M.M, (2000). Multiple functional deficits in peripheral autonomic organs in mice lacking muscarinic acetylcholine receptor gene for the M_3 subtype. *PNAS,* **97,** 9579–9584.

MCCONNELL, H.M., OWICKI, J.C., PARCE, J.W., MILLER, D.L., BAXTER, G.T., WADA, H.G. & PITCHFORD, S. (1992). The Cytosensor microphysiometer: biological applications of silicon technology. *Science,* **257,** 1906–1912.

MELOY, T.D., DANIELS, D.V., HEGDE, S.S., EGLEN, R.M. & FORD, A.P.D.W. (1998). Functional characterization of muscarinic cholinoceptors in rat submaxillary gland (RSG) using microphysiometry. *FASEB J.,* **12,** A441.

MORIYA, H., TAKAGI, Y., NAKANISHI, T., HAYASHI, M., TANI, T. & HIROTSU, I. (1999). Affinity profiles of various muscarinic antagonists for cloned human muscarinic acetylcholine receptor (mAChR) subtypes and mAChRs in rat heart and submandibular gland. *Life Sci.,* **64,** 2351–2358.

NORTON, P., KARRAM, M., WALL, L.L., ROSENZWEIG, B., BENSON, J.T. & FANTL, J.A. (1994). Randomized double-blind trial of terodiline in the treatment of urge incontinence in women. *Obstet. Gynecol.,* **84,** 386–391.

OWENS, R.G. & KARRAM, M.M. (1998). Comparative tolerability of drug therapies used to treat incontinence and enuresis. *Drug Safety,* **19,** 123–139.

VALDEZ, I.H. & TURNER, R.J. (1991). Effects of secretagogues on cytosolic Ca^{2+} levels in rat submandibular granular ducts and acini. *Am. J. Physiol.,* **261,** G359–G363.

WATSON, N., DANIELS, D.V., FORD, A.P.D.W., EGLEN, R.M. & HEGDE, S.S. (1999). Comparative pharmacology of recombinant human M_3 and M_5 muscarinic receptors expressed in CHO-K1 cells. *Br. J. Pharmacol.,* **127,** 590–596.

YARKER, Y.E., GOA, K.L. & FITTON, A. (1995). Oxybutynin. A review of its pharmacodynamic and pharmacokinetic properties, and its therapeutic use in detrusor instability. *Drug Aging,* **6,** 243–262.

YEOMANS, J., TAKEUCHI, J., JIA, Z., FULTON, J., ABRAMOV-NEWERLY, W., JAMOT, L. & RODER, J. (1999). Gene-targeted mice lacking M_5 receptors: genotypes and behavior. *Life Sci.,* **64,** 69 (abstract).

(Received August 7, 2000
Revised January 22, 2001
Accepted January 22, 2001)